GUIDED WAVE OPTICAL RF SPECTRUM ANALYZER

D. Mergerian, E.C. Malarkey, R.P. Pautienus, J.C. Bradley, A.L. Kellner and M.D. Mill
Westinghouse Systems Development Division, Advanced Technology Laboratory
Post Office Box 1521, Mail Stop 3714
Baltimore, Maryland 21203

ABSTRACT

The design, fabrication and performance of an integrated optical R.F. spectrum analyzer is described. The device consists of an injection laser, the IO substrate and a photodiode array. It operates over a frequency bandwidth of 400 MHz centered at 600 MHz and with a complete frame time of 2 μsec. An R.F. input signal dynamic range in excess of 20 dB has been measured.

Introduction

Over the past several years workers in the field of integrated optics have been striving to develop an integrated optical (I.O.) circuit for spectral analysis of R.F. signals.[1,2,3] This work was originally directed toward the development of specific I.O. components which were later to be integrated to form the functioning device. The components included planar optical waveguides, waveguide (geodesic) lenses,[4,5,6,7] surface acoustic wave (SAW) transducers,[8,9,10] an array of linear detectors[11,12] and an injection laser source.[13] These various components are discussed in the sections that follow together with a description of the overall system performance; the closing paragraph of this section briefly outlines the function of an integrated optical R.F. spectrum analyzer (I.O.S.A.)

The operation of an I.O.S.A. was first described by Hamilton,[1] et al, and an illustration of such a device appears in Figure 1.

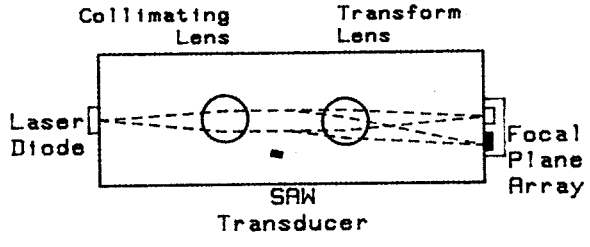

Fig. 1 Schematic of the Layout Used in the Integrated Optical R.F. Spectrum Analyzer

This injection laser output is located at the focal point of the first geodesic lens; the light is coupled into the waveguide and collimated by the first lens. The SAW transducers spatially modulate the guided optical beam, and the resulting deflected beam is focused by the second geodesic lens onto the output edge of the optical waveguide. A photodiode array that is butt-coupled to the waveguide edge detects the deflected beam. The beam's deflection angle is proportional to the frequency of the R.F. signal, and, in this way, the frequency of an incoming signal can be determined from the position of the focused beam on the detector array.

Waveguides

The spectrum analyzer was fabricated on X-cut $LiNbO_3$ with the c-axis parallel to the acoustic propagation. The optical waveguide was formed by diffusing 280Å of titanium into $LiNbO_3$ for 6 hours at 1000°C. This procedure resulted in a tightly confined optical beam that exhibited low-loss and allowed for good geodesic lens performance and efficient acoustooptic coupling. Both the input and output edges of the $LiNbO_3$ substrate are accurately polished to produce sharp, chip-free surfaces for effective input and output coupling.

Measurements made in these single mode waveguides indicate a propagation loss of 0.5 to 0.6 dB/cm and a scattered light level that is 55 dB below the peak transmitted beam intensity at an angle of less than one degree from the optical axis.

Geodesic Lenses

The geodesic lenses are axially symmetric aspherical depressions in the surface of the waveguide. A variational scheme based on ray optics was used to design these lenses.[4] The desired aspheric surfaces were machined by single-point diamond turning.[14] In particular:

1. The lenses can be precisely located on the substrate and thereby allow the focal plane for the system to be predetermined.
2. The lens profile can be maintained to better than 0.5 μm and this provides for diffraction limited performance.
3. The cut surface is very smooth and requires little or no polishing.

Measurements indicate that diamond machined geodesic lenses are indeed diffraction limited, have an insertion loss of 2-2.5 dB and have a focal plane within ± 2 μm of its intended position at the polished waveguide edge.

Performance of Truncated Gaussian Beams

Adequate performance of the spectrum analyzer requires that the focused beam exhibit significant side-lobe suppression in the focal plane. To assist in modeling side-lobe structure, a computer program has been written to calculate Fourier transforms of optical beams of arbitrary spatial and intensity profiles. This program obtains a curve-fitted representation of the beam profile as a linear combination of splines where each spline is a convolution product of a rectangular function; then the Fourier transform is accurately computed as a linear combination of pointwise products of sinc functions. Specific Fourier transforms found in the literature agree very well with results obtained from this program.[15,16]

0149-645X/81/0000-0517$00.75

Typical results of particular interest were obtained using this computer program, and they are illustrated in Figures 2 - 4. Figure 2 represents a Gaussian beam width of 2.0 mm that passes through a 3.3 mm aperture. The intensity profile in the focal plane is illustrated in Figure 3 and it is displayed over an array of individual detectors. Figure 4 shows similar results where the beam is that illustrated in Figure 2 with an offset of 400 μm (see dashed curve in Figure 2).

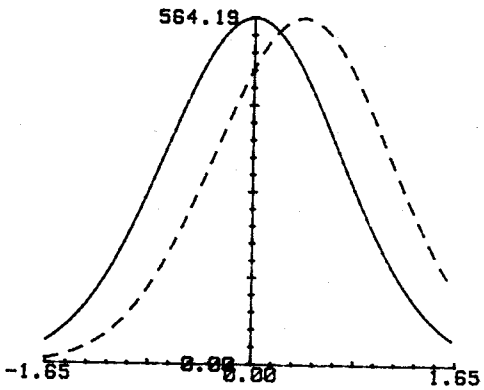

Fig. 2 Truncated Input Gaussian Beams

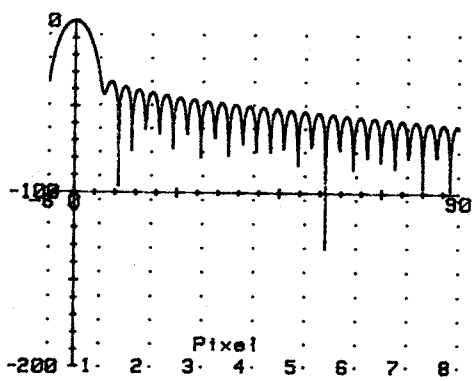

Fig. 3 Normalized Intensity (in dB) at Focal Plane

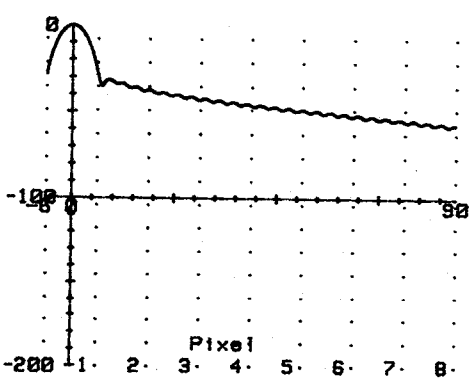

Fig. 4 Normalized Intensity (in dB) at Focal Plane for a 400 μm Offset

These results indicate that sufficient side-lobe suppression can be achieved for beam profiles and lens apertures used in the Westinghouse I.O.S.A.

System Performance

CW and long pulse operations have been used to evaluate the frequency and optical resolution, the total R.F. bandwidth and the system dynamic range. Pulses of shorter duration were used also to test the system response and to test its ability to handle two simultaneous signals. These tests were performed using an end-fire-coupled He-Ne laser source. Recently a GaAlAs diode laser has been successfully butt-coupled to the $LiNbO_3$ substrate. Results of this fully integrated system are forthcoming.

The dynamic range of the IO SA has been estimated by two different methods one direct and the other indirect. In the direct approach, the sweeping RF input signal of 40 to 80 mW is applied to the analyzer through a calibrated attenuator which can be varied in 1 dB steps. The signal from a representative, but arbitrarily chosen, photodiode is passed through a sample and hold circuit and displayed on an oscilloscope. Attenuation is inserted into the line until the signal can no longer be distinguished from the noise and then removed until the signal is equal to the noise. The RF dynamic range determined in this manner has been observed to vary between 18 and 22 dB.

The indirect method compares the maximum observed signal from any selected pixel to the minimum detectable signal estimated for the array. Peak signals ranging between 30 and 60 mV and minimum detectable signals of 70 to 80 μV are the most representative results. The ratios of these signals correspond to a maximum signal dynamic range of 26 to 29 dB.

The peak attainable output signals from the detector have been limited by input power limitations on both the optical and the RF sources. At the same time, the minimum detectable signal has been that observable with the instruments being employed, and it is not as low as the NES of the array. It is quite likely, therefore, that the dynamic range achievable with the IO SA in its current state of development is considerably greater than either of the above estimates would indicate.

Results of short-duration pulse tests in both the single and double pulsed mode are readily observable on an oscilloscope when the pulser and detector readout circuitry are running independently, but all attempts to synchronize the two so that data for single integration periods can be collected have been unsuccessful.

Single pulses of duration ranging between 30 and 0.3 μsec present no detection problem. At the 30 μsec end, the detector threshold performance is similar to that of the CW case. As the pulse duration decreases below the detector integration time, the apparent magnitude of the signal decreases as expected and the interpulse reproducibility degrades as different fractions of the pulse are sampled during each integration period. In one series of tests, RF powers of up to a watt or more were applied for $\geq$ 1 μsec durations with resultant detector output signals well in excess of 100 mV, thus indicating that a considerable response range beyond those seen in CW tests is still available.

Further Improvements

Additional work is being done on individual component designs and implementation to improve the operating performance of the I.O.S.A. Currently a new computer program is being developed to design lenses with a minimum power loss. Also, off chip noise subtraction techniques are being designed and low noise large signal preamplifiers have been built to improve the dynamic range at the I.O.S.A.

One characteristic of photodiode detection as employed in the Westinghouse detector chip, is a substantial fixed pattern output noise. In order to utilize the large dynamic ranges afforded by photodiode detection, this fixed pattern noise must be subtracted from the output of the detector. During feasability tests of the I.O.S.A. This subtraction was performed by the display computer. A more desirable off chip analog subtraction technique is now being developed which can be performed during every 2 μsec integration time. This method, using a track and hold analog memory, is expected to increase processing speed and dynamic range of the device. These efforts are directed toward designing extremely low noise, large dynamic range off-chip analog processing.

References

1. M.C. Hamilton, D.A. Wille and W.J. Miceli, "An Integrated Optical R.F. Spectrum Analyzer," 1976 Ultrasonic Symposium Proceedings, IEEE Cat. #76CH-1120-5SU, New York, 1976, pp. 218-222.

2. D.B. Anderson, J.T. Boyd, M.C. Hamilton and R.R. August, IEEE J. Quantum Electron., vol. QE-13, pp. 268-275, April 1955.

3. D. Mergerian, E.C. Malarkey, G.E. Marx, J.C. Bradley and R.P. Pautienus, Paper 13.2, 1979 Conference on Laser Engineering and Applications, Digest, pp. 78-79, (1979).

4. J.C. Bradley, E.C. Malarkey, D. Mergerian and H.A. Trenchard, Proc. Soc. Photo-Opt. Instrum. Eng., vol. 176, pp. 75-84, (1979).

5. S. Sottini, V. Russo and G.D. Righini, J. Opt. Soc. Am., vol. 69, p. 1248, (1979).

6. G.E. Betts, J.C. Bradley, G.E. Marx, D.C. Schubert and H.A. Trenchard, Appl. Opt., vol. 17, pp. 2346-2351 (1978).

7. D.W. Vahey and V.E. Wood, IEEE J. Quantum Electron., vol. QE-13, p. 129 (1977).

8. W.R. Smith, H.M. Gerard, J.H. Collins, T.M. Reader and H.J. Shaw, Invited Paper, MTT Trans., vol. MTT-17, pp. 865-873 (1979).

9. C.S. Tsai, M.A. Alhaider, L.T. Nguyen and B. Kim, IEEE Proc., vol. 64, pp. 318-328 (1976).

10. D. Mergerian, E.C. Malarkey, B. Newman, J. Lane, R. Weinert, B.R. McAvoy and C.S. Tsai, Ultrasonics Conference, Proceedings, IEEE Cat. #78CH-1344, 1SU, New York, 1978, pp. 64-69.

11. G.E. Marx and G.M. Borsuk, Paper ME6, 1980 Topical Meeting on Integrated and Guided-Wave Optics, Technical Digest, 1980.

12. G.M. Borsuk, IEEE Proc., vol. 69, pp. 100-118, January 1981.

13. For an extensive review of recent injection laser developments, see R.W. Dixon, BSTJ, vol. 59, pp. 669-722, May 1980.

14. D. Mergerian, E.C. Malarkey, R.P. Pautienus and J.C. Bradley, Proc. Soc. Photo-Opt. Instrum. Eng., vol. 176, p. 85, (1979).

15. P. Jacquinot and B. Roizen-Dossier, "Apodisation," Progress in Optics, vol. III, Ch. II., E. Wolf ed., John Wiley, New York, 1964.

16. D.L. Hecht, Optical Eng., vol. 16, p. 461 (1977).